THE JOURNAL OF PHYSICAL CHEMISTRY B

Article

pubs.acs.org/JPCB

Anisotropic Dielectric Relaxation of the Water Confined in Nanotubes for Terahertz Spectroscopy Studied by Molecular Dynamics Simulations

Wenpeng Qi,[†] Jige Chen,[†] Junwei Yang,[†,‡] Xiaoling Lei,[†] Bo Song,*[,†] and Haiping Fang[†]

[†]Shanghai Institute of Applied Physics, Chinese Academy of Sciences, P.O. Box 800-204, Shanghai 201800, China

[‡]College of Physical Science and Technology, Sichuan University, Chengdu 610064, P.R. China

ABSTRACT: The dynamics and structure of the hydrogen-bond network in confined water are of importance in understanding biological and chemical processes. Recently, terahertz (THz) time domain spectroscopy was widely applied for studying the kinetics of molecules and the hydrogen-bond network in water. However, the characteristics of the THz spectroscopy varying with respect to the confinement and the mechanism underlying the variation are still unclear. Here, on the basis of molecular dynamics simulations, the relationship between the anisotropic dielectric relaxation and the structure of the water confined in a carbon nanotube (CNT) was investigated. The results show that there are two preferred hydrogen-bond orientations of the confined water in the nanotube: (1) parallel to the CNT axis and (2) perpendicular to the CNT axis, which are clearly different. Moreover, the response of the orientations to the increment of the CNT diameters is opposite, leading to the opposite variations of the dielectric relaxation times along the two directions. The anisotropy in the relaxation time can be presented by the anisotropic dielectric permittivity which is able to be observed through THz spectroscopy. The anormal behaviors above are attributed to the special structure of the water close to the nanotube wall due to the confinement and hydrophobicity of CNT. These studies contribute an important step in understanding the THz experiments of water in nanoscales, and designing a chamber for specific chemical and biological reactions by controlling the diameters and materials of the nanotube.

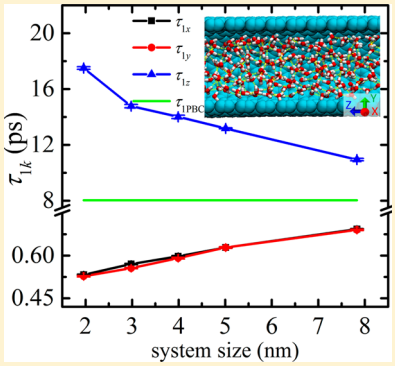

INTRODUCTION

The hydrogen-bond network governs the properties of water,[1] which plays an important role in chemical and biological reactions. Wang et al. have found that the special hydrogen-bond network could induce the interfacial water hydrophobic.[2,3] Tu et al. presented the amplification of the water dipole signal by the hydrogen-bond network.[4] Interestingly, it was revealed that the switch of the water flow in nanochannels could be realized on the basis of the continuity of hydrogen bonds.[5] For the case of the chemical and biological reactions, Relph et al. found that the special hydrogen-bond network could control proton-coupled water activation in HONO formation.[6] Additionally, it was reported that the water hydrogen-bond network played a catalytic role in photosynthetic oxygen evolution.[7,8] Qi et al. have presented metastable structures in the DNA hybridization process mediated by the hydrogen bond.[9]

Recently, terahertz time-domain spectroscopy (THz-TDS) provided a powerful noncontact method,[10−12] which can be used in detecting the dynamics of hydrogen-bond network formed by water molecules confined in nanoscaling space, due to the strong absorption of water molecules at the terahertz (THz) spectrum.[13,14] In 2001, using THz-TDS, Boyd and coworkers observed THz surface modes in nanometer-sized liquid water pools.[15] Liu et al. have studied super-cooled water confined in nanoporous silica materials by THz-TDS and simulations.[16] Tan et al. studied the reorientation dynamics of water in confined nanometer-sized micelles by ultrafast infrared polarization and molecular dynamics simulations.[17,18] They found that the orientational anisotropy data for three water nanopool sizes (4.0, 2.4, and 1.7 nm) can be fitted well with biexponential decays. The experimentally determined frequency−frequency correlation functions suggest that the confined water dynamics is substantially slower than bulk water dynamics and is size dependent. Turton et al. showed that water can be locked up in nanopools or worm-like structures using aqueous LiCl salt solutions and can be studied with THz spectroscopies.[19] Laage et al. studied the reorientation dynamics of nanoconfined water in hydrophobic silica pores by molecular dynamics simulations.[20] Skinner et al. have studied in detail the vibrational spectroscopy of water at liquid−vapor and liquid−solid interfaces.[21]

Although all of the works mentioned above focus on the THz spectroscopy of water confined in nanoscaling space, the characteristics of the spectroscopy varying with respect to the confinement and the mechanism underlying the variation are still unclear.

Received: December 7, 2012
Revised: June 9, 2013
Published: June 10, 2013

Here, we performed the molecular dynamics (MD) simulations of water molecules confined in carbon nanotubes (CNTs) with different diameters, and then calculated the dielectric permittivity of THz spectroscopy for the confined water. A bimodal relaxation time distribution involving two Debye processes was used to fit the permittivity. We observed that the dielectric relaxation time of the slow process (the cooperative relaxation) for the confined water was anisotropic clearly, while the dielectric relaxation time of the fast process (the fast reorientation of mobile water molecules) was not. The mechanism underlying the anisotropy is the preferred hydrogen-bond orientations of the confined water in the nanotube, which can change the kinetics of the hydrogen-bond network, and subsequently cause the difference of the dielectric relaxation times along the different directions. These studies contribute an important step in understanding the THz experiments of water in nanoscale and designing a chamber for specific chemical and biological reactions by controlling the diameters and materials of the nanotube.

SIMULATION METHODS

Five uncapped [(25, 0), (38, 0), (51, 0), (64, 0), (100, 0)] zigzag single-walled nanotubes (SWNTs) with diameters of 1.96, 2.98, 3.99, 5.01, and 7.83 nm and the same length of 4.26 nm were immersed in water. The dimensions of the water boxes for the SWNTs were 5.00 × 5.00 × 6.00, 6.00 × 6.00 × 6.00, 7.00 × 7.00 × 6.00, 8.00 × 8.00 × 6.00, and 10.00 × 10.00 × 6.00 nm^3, respectively. The nanotube axis is along the z direction. The systems were equilibrated for 5 ns under the NPT conditions with a constant pressure of 1 bar and a constant temperature of 300 K. After that, there are 254, 723, 1429, 2310, and 6105 water molecules entering the five nanotubes, respectively. The SWNTs and the water molecules confined in the nanotubes were extracted from the boxes above, and then were aligned along the z axis in new periodic boxes with the length in the z direction equaling the length of the nanotubes, namely, 5.00 × 5.00 × 4.32, 6.00 × 6.00 × 4.32, 7.00 × 7.00 × 4.32, 8.00 × 8.00 × 4.32, and 11.00 × 11.00 × 4.32 nm^3, respectively (Figure 1). In this way, we got the water confined in the nanotube, while the vacuum between two nanotubes in x and y directions is more than 3 nm. These systems were simulated under NVT conditions with a constant temperature of 300 K. Water in a box of 5.00 × 5.00 × 5.00 nm^3 with periodic boundary conditions, as a reference to the water confined in nanotubes, was performed under the NPT conditions (a constant pressure of 1 bar and a constant temperature of 300 K).

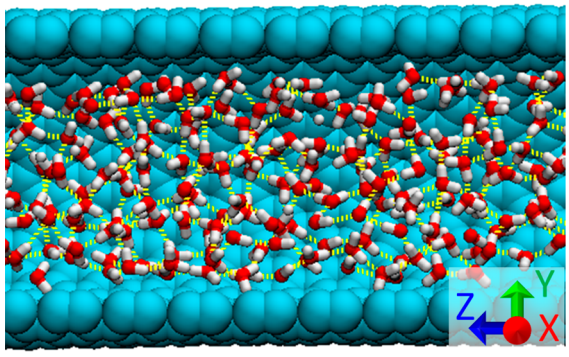

Figure 1. Snapshot of the confined water in the SWNT with a diameter of 1.96 nm. In order to demonstrate the water molecules within the nanotube, half of the nanotube is not shown. The cyan ball denotes the carbon atom of the nanotube, while the red and white balls stand for oxygen and hydrogen atoms of water molecules, respectively. The lime dashed line indicates the hydrogen bond between water molecules.

All the simulations were performed with Gromacs-4.5.[22] The water molecule was modeled by SPC/E,[23] which has been used widely for liquid properties of water.[24−27] The Parrinello−Rahman[28] and the Nosé−Hoover[29] methods were applied for keeping the system at a constant pressure and a constant temperature, respectively. The time step was 1 fs, and the data were collected every 0.1 ps. In the simulations, carbon atoms were modeled as uncharged Lennard-Jones particles with a cross section of δ_{CC} = 3.40 Å, δ_{CO} = 3.33 Å, and a potential well depth of ε_{CC} = 0.36 kJ/mol, ε_{CO} = 0.48 kJ/mol.[30] The carbon−carbon bond lengths of 1.40 Å and bond angles of 120° were maintained by harmonic potentials. The linear and angular spring constants were set at 3.94 × 10^6 kJ·mol^{-1}·$Å^{-2}$ and 527.00 kJ·mol^{-1}·deg^{-2}, respectively. A cutoff of 1 nm was applied for the Lennard-Jones interaction and the real space portion of the electrostatic interaction, while the PME method was used for the reciprocal space portion of the electrostatic interaction.[31] For each system, the simulation was performed for 110 ns with the last 100 ns sampled for analysis. Because the largest system contains more than 20 000 atoms, a long-time simulation is needed to equilibrate the total dipole moment. The standard error of the results was calculated on the basis of evenly dividing the last 100 ns trajectory into independent 10 blocks.

RESULTS AND DISCUSSION

The confinement of the nanotube is anisotropic. Subsequently, the dielectric permittivity of water confined in the nanotube is anisotropic. The THz pulse is electromagnetic waves vibrating along the direction vertical to the propagation direction. If the incident THz pulses propagate along the z axis in the confined water systems, the measurement of the THz-TDS is determined by the permittivity in the direction perpendicular to the z axis. If the THz pulses propagate along the x (y) axis, the results of THz-TDS are contributed by the permittivity in the direction perpendicular to the x (y) axis.

For a linearly polarized THz pulse, the dielectric permittivity in the k direction $\varepsilon_k(\nu)$ was calculated by the following equation:[32,33]

$$\frac{\varepsilon_k(2\pi\nu) - {n_{\infty k}}^2}{4\pi} = \frac{1}{3k_BTV}[\langle P_k(0)\rangle^2 + \int \mathrm{d}t e^{i2\pi\nu t}[\mathrm{d}C_k(t)/\mathrm{d}t]] \quad (1)$$

$$C_k(t) = \frac{\langle P_k(t)\cdot P_k(0)\rangle}{\langle P_k(0)\cdot P_k(0)\rangle} \quad (2)$$

with $k = x$, y, and z. $P_k = \vec{P}\cdot\vec{n}_k$; the vector $\vec{P}$ is the total dipole moment of the system, which can be obtained directly from the MD simulations, and $\vec{n}_k$ is the unit vector along the k direction which is parallel to the THz polarization direction. $C_k(t)$ is the total dipole moment autocorrelation function. T is the temperature, k_B is the Boltzmann constant, V is the inner volume of the nanotube, ν is the frequency, and $n_{\infty k}$ is the refractive index at infinitely high frequency. The $\varepsilon_k(2\pi\nu) = \varepsilon'_k(2\pi\nu) + i\varepsilon''_k(2\pi\nu)$ of the water confined in nanotubes for the

dx.doi.org/10.1021/jp3120435 | J. Phys. Chem. B 2013, 117, 7967−7971

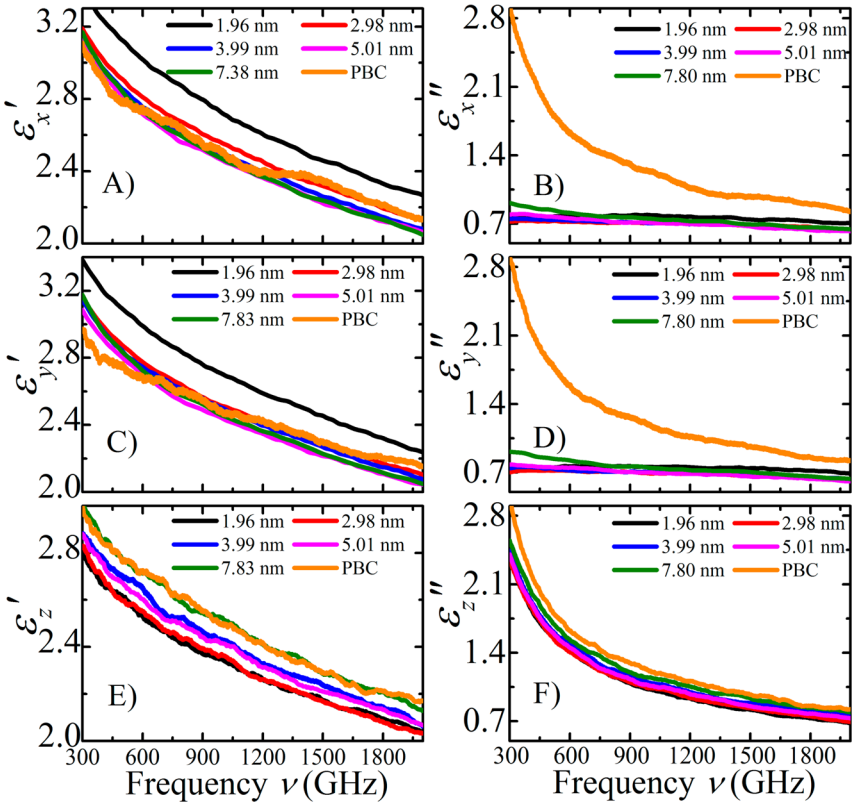

Figure 2. Dielectric permittivity of the water confined in the nanotubes with different diameters (1.96, 2.98, 3.99, 5.01, and 7.83 nm). (A and B), (C and D), (E and F) The permittivity in the *x*, *y*, and *z* directions, respectively. The label of PBC denotes the water in a box with periodic boundary conditions as a reference system. The standard errors of the permittivities for the water in the nanotubes along the *x*, *y* directions are $\pm 7.9 \times 10^{-3}$, while the standard errors for the water in the nanotubes along the *z* direction and the bulk water along the *x*, *y*, and *z* directions are ± 0.15.

THz polarization direction along the *x*, *y*, and *z* axis are shown in Figure 2. The imaginary parts of the permittivities in the *x*, *y* directions are clearly different from the imaginary part in the *z* direction. These behaviors are related to the anisotropy of the nanotubes.

To illuminate the mechanism under the anisotropic behavior of the permittivity, the real and imaginary parts of the complex permittivity were fitted by the distribution of bimodal relaxation time which involves two Debye processes (τ_{1k}, τ_{2k})

$$\varepsilon_k(2\pi\nu) = \varepsilon_k'(2\pi\nu) + i\varepsilon_k''(2\pi\nu) = \frac{\varepsilon_{1k} - \varepsilon_{2k}}{1 + i2\pi\nu\tau_{1k}} + \frac{\varepsilon_{2k} - \varepsilon_{\infty k}}{1 + i2\pi\nu\tau_{2k}} + \varepsilon_{\infty k} \quad (3)$$

where ε_{1k} is the static permittivity in the *k* direction, ε_{2k} is the intermediate frequency dielectric constant in the *k* direction. $\varepsilon_{1k} - \varepsilon_{2k}$ and $\varepsilon_{2k} - \varepsilon_{\infty k}$ are the amplitudes of the two individual processes, respectively, while $\varepsilon_{\infty k}$ is the permittivity with infinitely high frequency along the *k* direction. The slow process, characterized by a large dielectric relaxation time τ_{1k}, is usually attributed to the cooperative relaxation specifically for hydrogen-bond liquids, which arises from long-range hydrogen-bond-mediated dipole−dipole interactions.[34] The fast process, labeled by a small dielectric relaxation time τ_{2k}, is usually attributed to the fast reorientation of mobile water molecules which have only one hydrogen bond or no hydrogen bond within the local network of hydrogen-bonded molecules.[35]

The dielectric relaxation times in the *x*, *y*, and *z* directions with respect to the SWNT diameter are presented in Figure 3. Obviously, for the slow process, as the diameter increases, τ_{1z} decreases, while $\tau_{1x} \approx \tau_{1y}$ increases. These indicate the remarkable effect of the anisotropic confinement on the slow process. The variation of the relaxation time τ_{2k} for the fast process in the *x*, *y*, and *z* directions is very weak (the inset in Figure 3), meaning that the impact of the nanotube diameter on the fast process is weak. The difference of the relaxation time τ_2 between the *x*, *y* directions and the *z* direction is attributed to the hydrophobicity of the SWNT wall in the radical direction and the hydrophilicity in the axial direction.

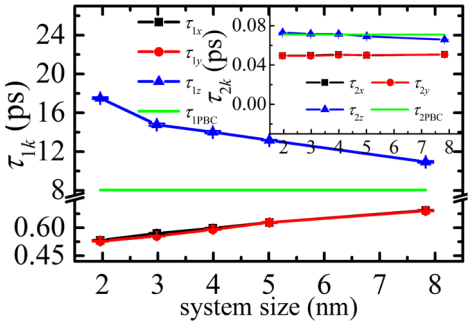

Figure 3. Dielectric relaxation time of the slow process in *x*, *y*, and *z* directions, τ_{1x} (black), τ_{1y} (red), and τ_{1z} (blue), of the water confined in nanotubes with respect to the increment of the nanotube diameters. The inset shows the dielectric relaxation time of the fast process in *x*, *y*, and *z* directions, τ_{2x} (black), τ_{2y} (red), and τ_{2z} (blue). The green line is the relaxation time τ_{2PBC} of the water in a box with periodic boundary conditions as a reference system.

The relaxation time, τ_1, of the slow process relates to the orientation of hydrogen bonds. The hydrogen bond between

dx.doi.org/10.1021/jp3120435 | J. Phys. Chem. B 2013, 117, 7967−7971

two water molecules was specified if the O−O distance was less than 3.50 Å and the angle H−O···O was less than 30° simultaneously. The orientational distribution probability of hydrogen bonds, P, was calculated by the following formula:

$$P = C\frac{N(\theta)}{\sin\theta} \tag{4}$$

where C is the normalized coefficient and $N(\theta)$ is the number of hydrogen bonds with a angle θ between the z axis and the hydrogen-bond vector. The hydrogen-bond vector is defined from the oxygen atom of the first water molecule as a donor providing the hydrogen atom in a hydrogen bond to the oxygen atom of the second water molecule as an acceptor accepting the hydrogen atom. The results are presented in Figure 4. There

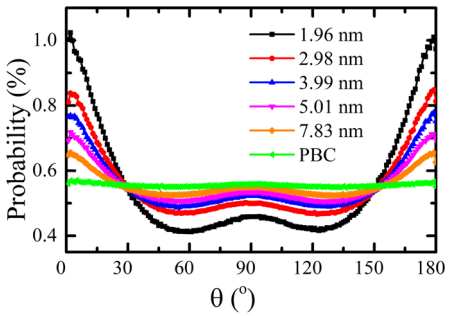

Figure 4. Probabilities of hydrogen bond orientation of the water confined in the nanotubes with diameters of 1.96 nm (black), 2.97 nm (red), 3.99 nm (blue), 5.01 nm (magenta), and 7.83 nm (orange) and the water in a box with periodic boundary conditions (green). The standard errors of the probabilities are $\pm 1.9 \times 10^{-5}$.

are three peaks in the probability at 0, 90, and 180°, respectively. Thus, two preferred orientations occur for the confined water: (1) the direction parallel to the z axis (the peaks at 0 and 180°) and (2) the direction perpendicular to the z axis (the peak at 90°), which is clearly different from bulk water with no preferred orientation of hydrogen bonds. Due to more hydrogen bonds mediating the dipole−dipole interactions in the direction of the preferred orientation, the dipole−dipole interaction is stronger than the interaction in other directions, which leads to the dipole moments along this direction being more stable than the dipole moments along the other directions. As the increment of the nanotube diameters, the probability of hydrogen-bond orientations parallel to the nanotube axis decreases (Figure 4), which induces the decrease of the dipole-moment stability, and then results in the decrease of the relaxation time τ_{1z} (Figure 3). On the contrary, as the increment of the nanotube diameters, the probability of the hydrogen-bond orientations increases in the direction perpendicular to the nanotube axis, resulting in the relaxation times τ_{1x} and τ_{1y} in the radial direction increasing. Therefore, the preferred hydrogen-bond orientation of the confined water in the nanotube plays a key role in the slow relaxation process.

These preferred orientations can be attributed to the confinement and hydrophobicity of the carbon nanotube. The water molecules cannot form hydrogen bonds with the hydrophobic nanotube. Therefore, the hydrogen-bond orientations of the water close to the nanotube wall are mainly confined along the axial direction, resulting in the strong peak of the orientation distribution at 0 and 180°. This also leads to the weak peak of the distribution at 90°, considering the 109.5° angle between two OH bonds of a water molecule H_2O. Therefore, the hydrogen-bond orientations along the axial direction of the nanotube are more stable than the orientations along the radial direction, which results in the dielectric relaxation time along the axial direction (τ_{1z}) is clearly larger than the relaxation time along the radial directions (τ_{1x}, τ_{1y}) in Figure 3.

Finally, it is noted that the SWNT wall can prevent the formation of the hydrogen bonds between the water molecules inside and outside. The distance between two water molecules connected by a hydrogen bond was about 0.29 nm, and the interaction energy between them was about 21 kJ/mol. When the SWNT wall was inserted between the two water molecules, the distance of them became about 0.64 nm. Considering the dipole−dipole interaction follows an inverse cubic law, the interaction energy of the two water molecules with the nanotube wall between them can be estimated to be less than 2 kJ/mol, similar to the thermal fluctuations about 3 kJ/mol at T = 300 K. Therefore, the collective effect of water molecules outside the nanotube will play a very weak role on our observations, and the main results of the simulations will remain if the SWNTs are immersed in water.

CONCLUSION

In summary, the relationship between the anisotropic dielectric relaxation and the structure of the water confined in SWNTs was investigated on the basis of the MD simulations. The confinement of the nanotube induces two preferred hydrogen-bond orientations, parallel and perpendicular to the nanotube axis, which are clearly different. Additionally, with the increase of nanotube diameter, the responses of these two preferred orientations are opposite, which leads to the opposite responses in the cooperative relaxation of the water, and then results in the anisotropic behavior of the dielectric relaxation times and the observable dielectric permittivity in the THz-TDS experiment. These findings contribute an important step in understanding the THz-TDS results of the confined water in nanoscales.

AUTHOR INFORMATION

Corresponding Author

*E-mail: bosong@sinap.ac.cn. Phone: -86-021-59554785. Fax: 86-21-39192394.

Notes

The authors declare no competing financial interest.

ACKNOWLEDGMENTS

We acknowledge Profs. Junichiro Shiomi and Hongwei Zhao and Drs. Niall English and YuSong Tu for their useful discussions. This work was supported by National Basic Research Program of China under Grant No. 2010CB934504, National Natural Science Foundation of China 11174310 and 60907044, Main Direction Program of Knowledge Innovation Program of Chinese Academy of Sciences, the Major Research Plan of National Natural Science Foundation of China 11290164, China Postdoctoral Science Foundation Project 2012M511159, and the Shanghai Supercomputer Center of China.

REFERENCES

(1) Franks, F. *Water, a Comprehensive Treatise*; Plenum: New York, 1972.

(2) Wang, C. L.; Lu, H. J.; Wang, Z. G.; Xiu, P.; Zhou, B.; Zuo, G. H.; Wan, R. Z.; Hu, J. Z.; Fang, H. P. Stable Liquid Water Droplet on a Water Monolayer Formed at Room Temperature on Ionic Model Substrates. *Phys. Rev. Lett.* **2009**, *103*, 137801.
(3) Wang, C. L.; Zhou, B.; Tu, Y. S.; Duan, M. Y.; Xiu, P.; Li, J. Y.; Fang, H. P. Critical Dipole Length for the Wetting Transition due to Collective Water-Dipoles Interactions. *Sci. Rep.* **2012**, *2*, 358.
(4) Tu, Y. S.; Xiu, P.; Wan, R. Z.; Hu, J.; Zhou, R. H.; Fang, H. P. Water-Mediated Signal Multiplication with Y-Shaped Carbon Nanotubes. *Proc. Natl. Acad. Sci. U.S.A.* **2009**, *106*, 18120−18124.
(5) Li, J. Y.; Gong, X. J.; Lu, H. J.; Li, D.; Fang, H. P.; Zhou, R. H. Electrostatic Gating of a Nanometer Water Channel. *Proc. Natl. Acad. Sci. U.S.A.* **2007**, *104*, 3687−3692.
(6) Relph, R. A.; Guasco, T. L.; Elliott, B. M.; Kamrath, M. Z.; McCoy, A. B.; Steele, R. P.; Schofield, D. P.; Viggiano, A. A.; Ferguson, E. E.; Johnson, M. A. How the Shape of an H-Bonded Network Controls Proton-Coupled Water Activation in HONO Formation. *Science* **2010**, *327*, 308−312.
(7) Polander, B. C.; Barry, B. A. A. Hydrogen-Bonding Network Plays a Catalytic Role in Photosynthetic Oxygen Evolution. *Proc. Natl. Acad. Sci. U.S.A.* **2012**, *109*, 6112−6117.
(8) Umena, Y.; Kawakami, K.; Shen, J. R.; Kamiya, N. Crystal Structure of Oxygen-Evolving Photosystem II at a Resolution of 1.9 Å. *Nature* **2011**, *473*, 55−U65.
(9) Qi, W. P.; Song, B.; Lei, X. L.; Wang, C. L.; Fang, H. P. DNA Base Pair Hybridization and Water-Mediated Metastable Structures Studied by Molecular Dynamics Simulations. *Biochemistry* **2011**, *50*, 9628−9632.
(10) Han, J. G.; Zhang, W. L.; Chen, W.; Thamizhmani, L.; Azad, A. K.; Zhu, Z. Y. Far-Infrared Characteristics of ZnS Nanoparticles Measured by Terahertz Time-domain Spectroscopy. *J. Phys. Chem. B* **2006**, *110*, 1989−1993.
(11) Zhang, S.; Park, Y. S.; Li, J. S.; Lu, X. C.; Zhang, W. L.; Zhang, X. Negative Refractive Index in Chiral Metamaterials. *Phys. Rev. Lett.* **2009**, *102*, 023901.
(12) Lu, X. F.; Zhang, X. C. Generation of Elliptically Polarized Terahertz Waves from Laser-Induced Plasma with Double Helix Electrodes. *Phys. Rev. Lett.* **2012**, *108*, 123903.
(13) Tielrooij, K. J.; Garcia-Araez, N.; Bonn, M.; Bakker, H. J. Cooperativity in Ion Hydration. *Science* **2010**, *328*, 1006−1009.
(14) Heyden, M.; Sun, J.; Funkner, S.; Mathias, G.; Forbert, H.; Havenith, M.; Marx, D. Dissecting the Thz Spectrum of Liquid Water from First Principles via Correlations in Time and Space. *Proc. Natl. Acad. Sci. U.S.A.* **2010**, *107*, 12068−12073.
(15) Boyd, J. E.; Briskman, A.; Colvin, V. L.; Mittleman, D. M. Direct Observation of Terahertz Surface Modes in Nanometer-Sized Liquid Water Pools. *Phys. Rev. Lett.* **2001**, *87*, 147401.
(16) Liu, L.; Faraone, A.; Mou, C.; Yen, C. W.; Chen, S. H. Slow Dynamics of Supercooled Water Confined in Nanoporous Silica Materials. *J. Phys.: Condens. Matter* **2004**, *16*, S5403−S5436.
(17) Tan, H. S.; Piletic, I. R.; Fayer, M. D. Orientational Dynamics of Water Confined on a Nanometer Length Scale in Reverse Micelles. *J. Chem. Phys.* **2005**, *122*, 174501.
(18) Tan, H. S.; Piletic, I. R.; Riter, R. E.; Levinger, N. E.; Fayer, M. D. Dynamics of Water Confined on a Nanometer Length Scale in Reverse Micelles: Ultrafast Infrared Vibrational Echo Spectroscopy. *Phys. Rev. Lett.* **2005**, *94*, 057405.
(19) Turton, D. A.; Corsaro, C.; Candelaresi, M.; Brownlie, A.; Seddon, K. R.; Mallamace, F.; Wynne, K. The Structure and Terahertz Dynamics of Water Confined in Nanoscale Pools in Salt Solutions. *Faraday Discuss.* **2011**, *150*, 493−504.
(20) Laage, D.; Thompson, W. H. Reorientation Dynamics of Nanoconfined Water: Power-Law Decay, Hydrogen-Bond Jumps, and Test of a Two-State Model. *J. Chem. Phys.* **2012**, *136*, 044513.
(21) Skinner, J. L.; Pieniazek, P. A.; Gruenbaum, S. M. Vibrational Spectroscopy of Water at Interfaces. *Acc. Chem. Res.* **2012**, *45*, 93−100.
(22) Hess, B.; Kutzner, C.; van der Spoel, D.; Lindahl, E. GROMACS 4: Algorithms for Highly Efficient, Load-Balanced, and Scalable Molecular Simulation. *J. Chem. Theory Comput.* **2008**, *4* (3), 435−447.
(23) Berendsen, H. J. C.; Grigera, J. R.; Straatsma, T. P. The Missing Term in Effective Pair Potentials. *J. Phys. Chem.* **1987**, *91*, 6269−6271.
(24) Starr, F. W.; Harrington, S.; Sciortino, F.; Stanley, H. E. Slow Dynamics of Water under Pressure. *Phys. Rev. Lett.* **1999**, *82*, 3629−3632.
(25) Starr, F. W.; Sciortino, F.; Stanley, H. E. Dynamics of Simulated Water under Pressure. *Phys. Rev. E* **1999**, *60*, 6757−6768.
(26) Anderson, J.; Ullo, J. J.; Yip, S. Molecular-Dynamics Simulation of Dielectric-Properties of Water. *J. Chem. Phys.* **1987**, *87*, 1726−1732.
(27) English, N. J.; Macelroy, J. M. D. Atomistic Simulations of Liquid Water Using Lekner Electrostatics. *Mol. Phys.* **2002**, *100*, 3753−3769.
(28) Parrinello, M.; Rahman, A. Polymorphic Transitions in Single-Crystals: a New Molecular-Dynamics Method. *J. App. Phys.* **1981**, *52*, 7182−7190.
(29) Nose, S. A. Unified Formulation of the Constant Temperature Molecular-Dynamics Methods. *J. Chem. Phys.* **1984**, *81*, 511−519.
(30) Duan, Y.; Wu, C.; Chowdhury, S.; Lee, M. C.; Xiong, G.; Zhang, W.; Yang, R.; Cieplak, P.; Kollman, P. A. Point-Charge Force Field for Molecular Mechanics Simulations of Proteins Based on Condensed-Phase Quantum Mechanical Calculations. *J. Comput. Chem.* **2003**, *24*, 1999−2012.
(31) Darden, T.; York, D.; Pedersen, L. Particle Mesh Ewald: an N•Log(N) Method for Ewald Sums in Large Systems. *J. Chem. Phys.* **1993**, *98*, 10089−10092.
(32) Lin, Y.; Shiomi, J.; Maruyama, S.; Amberg, G. Dielectric Relaxation of Water inside a Single-Walled Carbon Nanotube. *Phys. Rev. B* **2009**, *80*, 045419.
(33) Zasetsky, A. Y.; Lileev, A. S.; Lyashchenko, A. K. Molecular Dynamic Simulations of Terahertz Spectra for Water-Methanol Mixtures. *Mol. Phys.* **2010**, *108*, 649−656.
(34) Fukasawa, T.; Sato, T.; Watanabe, J.; Hama, Y.; Kunz, W.; Buchner, R. Relation between Dielectric and Low-Frequency Raman Spectra of Hydrogen-Bond Liquids. *Phys. Rev. Lett.* **2005**, *95*, 197802.
(35) Buchner, R.; Barthel, J.; Stauber, J. The Dielectric Relaxation of Water between 0 and 35 °C. *Chem. Phys. Lett.* **1999**, *306*, 57−63.